Thio- and Oxoflavopiridols, Cyclin-Dependent Kinase 1-Selective Inhibitors: Synthesis and Biological Effects

Kyoung Soon Kim,*[,§] John S. Sack,[†] John S. Tokarski,[†] Ligang Qian,[§] Sam T. Chao,[§] Leslie Leith,[§] Yolanda F. Kelly,[§] Raj N. Misra,[§] John T. Hunt,[§] S. David Kimball,[§] William G. Humphreys,[#] Barris S. Wautlet,[‡] Janet G. Mulheron,[‡] and Kevin R. Webster[‡]

Departments of Oncology Chemistry, Oncology Drug Discovery, Structural Biology and Modelling, and Metabolism and Pharmacokinetics, Bristol-Myers Squibb Pharmaceutical Research Institute, Princeton, New Jersey 08543-4000

Received June 5, 2000

Flavopiridol analogues, thio- and oxoflavopiridols which contain a sulfur (**16**) or oxygen (**18**) atom linker between a chromone ring and the hydrophobic side chain, are selective cyclin-dependent kinase 1 (CDK1) inhibitors with an IC_{50} of 110 and 130 nM. These analogues were prepared from key intermediate **7** by substituting the ethyl sulfoxide. Enantio pure intermediate piperidone **10** was obtained from the racemic piperidone **8** via a very efficient "dynamic kinetic resolution" in 76% yield. Hydrophobic side chains such as chlorophenyl or *tert*-butyl produced potent CDK1 inhibitory activity, while hydrophilic side chains such as pyrimidine or aniline caused a severe reduction in CDK inhibitory activity. These analogues are competitive inhibitors with respect to ATP, and therefore activity was dependent upon the CDK subunit without being affected by the cyclin subunit or protein substrate. Thio- and oxoflavopiridols **16** and **18** are not only selective within the CDK family but also discriminated between unrelated serine/threonine and tyrosine protein kinases. CDK1 selective thio- and oxoflavopiridol analogues inhibit the colony-forming ability of multiple human tumor cell lines and possess a unique antiproliferative profile in comparison to flavopiridol.

Introduction

The cyclin-dependent kinases (CDKs) are serine/threonine protein kinases which are the driving force behind the cell cycle and cell proliferation.[1,2] CDKs are multisubunit enzymes composed of at least a catalytic subunit (CDK) and a regulatory subunit (cyclin). To date at least 10 CDKs and 15 cyclins have been identified. Once activated, CDKs phosphorylate and modulate the activity of a variety of cellular proteins. These proteins can be categorized as tumor suppressors (e.g., RB, p53), transcription factors (e.g., E2F-DP, RNA pol II), replication factors (replication protein A), and organizational factors that influence cellular and chromatin structures (e.g., histone H1, lamin A, MAP4).[3] Individual CDKs perform distinct roles in cell cycle progression and can be classified as either G1, S, or G2/M phase enzymes.[1] The kinase activity of CDK complexes is tightly regulated and cell cycle-dependent. This regulation occurs at the level of cyclin gene transcription, cyclin protein degradation, and posttranslational modification of the CDK subunit. In addition, two families of CDK inhibitory proteins have been identified: the KIP proteins p21, p27, and p57 and the INK4 proteins p15, p16, p18, and p19.[4] Aberrations in each of these regulatory pathways have been found in a large percentage of human tumors including melanoma, lymphoma, and carcinomas of the breast, prostate, colon, non-small-cell lung, ovarian, pancreatic, and squamous cell.[5] As a result, there is considerable interest in restoring normal cell cycle control in tumor cells by targeting CDKs or CDK-associated molecules.[6]

Toward this end, several ATP-competitive small organic molecules have been reported in the literature as CDK inhibitors. Flavopiridol (**1**),[7] butyrolactone (**2**),[8] olomoucine (**3**),[9] and kenpaullone (**4**)[10] and subsequently several analogues[11] of olomoucine and flavopiridol have been reported. While butyrolactone (**2**) and olomoucine (**3**) inhibit both CDK1 and CDK2 without having appreciable CDK4 inhibitory activity, flavopiridol (**1**) is known to have a broad spectrum of CDK inhibitory activity against CDK1, -2, and -4 and is significantly less active against unrelated kinases (Table 3).

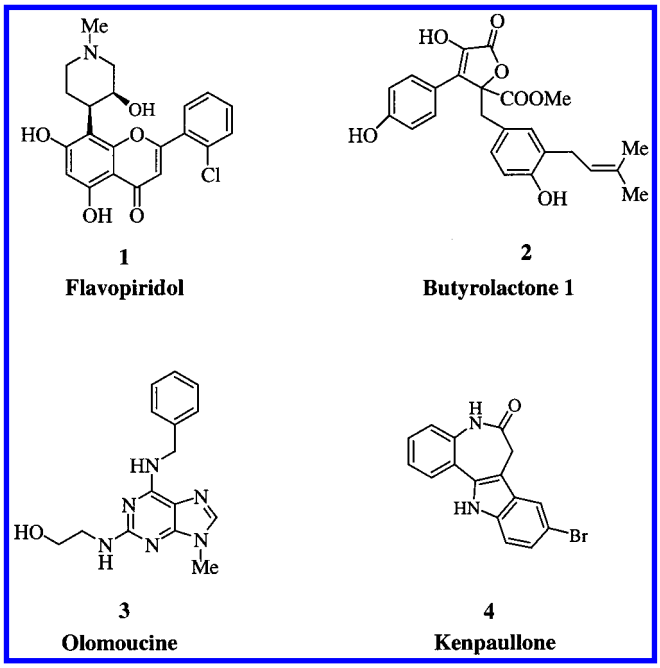

These attributes plus the fact that flavopiridol is a highly potent inhibitor of tumor cell proliferation make

* To whom correspondence should be addressed. Tel: (609) 252-5181. Fax: (609) 252-6601. E-mail: kyoung.kim@bms.com.
[§] Department of Oncology Chemistry.
[‡] Department of Oncology Drug Discovery.
[†] Department of Structural Biology and Modelling.
[#] Department of Metabolism and Pharmacokinetics.

10.1021/jm000231g CCC: $19.00
Published on Web 10/14/2000

Scheme 1

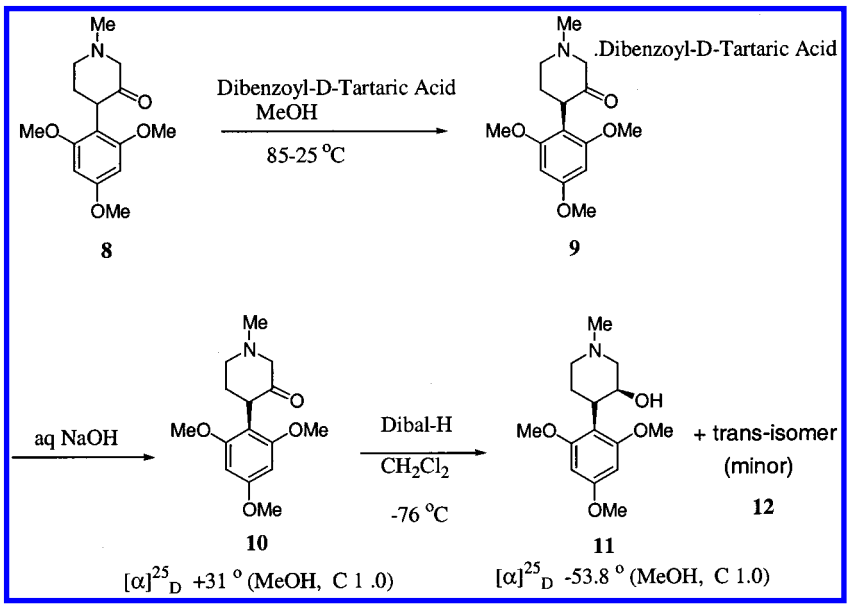

it an interesting target for further analogue synthesis. We set out to prepare analogues which would be more selective within the CDK family and possess a unique spectrum of antitumor activity. Herein, we report a series of thio- and oxoflavopiridols that are CDK1-selective inhibitors of the prototype **5** where the piperidylchromone ring is coupled to the hydrophobic R group via a sulfur or oxygen atom linker.

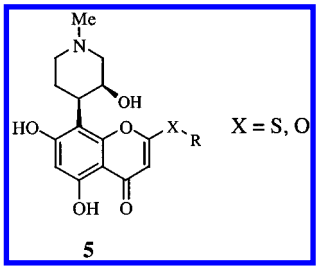

We originally envisioned that thioether **6** or alkyl sufoxide intermediate **7** would serve as a key intermediate. Replacement of the thioalkyl or alkyl sulfoxide group with the appropriate nucleophiles would expedite analogue synthesis.[12] Interestingly, the thio and oxo analogues (Nu = SR or OR) demonstrated CDK1-selective inhibitory activities and displayed unique biological properties, presumably due to an altered selectivity profile. The synthesis, structure−activity relationships (SARs), and biological properties of these compounds are described below.

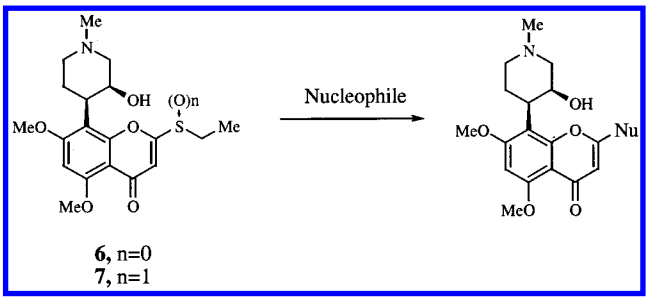

Chemistry

The key chiral intermediates for the analogue synthesis, thioether **6** and sulfoxide **7**, were prepared from chiral piperidone **10** which was obtained from racemic piperidone **8**[13] via a very efficient "dynamic kinetic resolution"[14] (Scheme 1). Heating racemic piperidone **8** in the presence of dibenzoyl-D-tartaric acid in methanol provides optically pure piperidone **10** in 76% yield after removing dibenzoyl-D-tartaric acid. Desired enantiomeric salt **9** was quite insoluble in methanol, while the opposite enantiomeric salt was soluble. There is a difference not only in solubility between these two diastereomeric salts but also in thermodynamic stability. The relative ratio of the two diastereomeric salts existing in hot methanol solution (not in the precipitates) was ca. 4:1 in favor of the desired enantiomeric salt **9** as determined by chiral HPLC column. We believe that a facile in situ epimerization of the C-4 chiral center under the reaction conditions, the thermodynamic stability difference between the two diastereomeric salts in favor of the desired 4*R*-enantiomer of piperidone **9**, and a large solubility difference between the two diastereomeric salts in methanol enable this "dynamic kinetic resolution" to be very efficient. Enantio pure piperidone **10** was prepared on 100-g scale by this process. Reduction of piperidone **10** using Dibal-H provided the mixture of *cis*-alcohol **11** (56% yield) and *trans*-alcohol **12** (13% yield) after purification.

Acylation, which produced concomitant demethylation, followed by treatment of **13** with carbon disulfide produced thiol **14** (Scheme 2). Depending on the nucleophiles, either thioether **6**, obtained by the ethylation of thiol **14**, or its diastereomeric mixture of sulfoxide **7** was used. Sulfoxide **7** generally led to the higher yields of the product under milder reaction conditions. Demethylation of thioether **15** produced the desired thioflavopiridol **16**. Analogues shown in Table 1 (**22**−**26**) were prepared in a similar manner using racemic intermediate thioethyl **19** or sulfoxide **20** (Scheme 3).

Results and Discussion

The biological activities of flavopiridol and thio-, oxo-, and other flavopiridol analogues were compared in a series of protein kinase and clonogenic (colony-formation) assays. As illustrated in Table 1, flavopiridol (**1**) is a potent, broad-spectrum inhibitor of CDKs. Ana-

Scheme 2

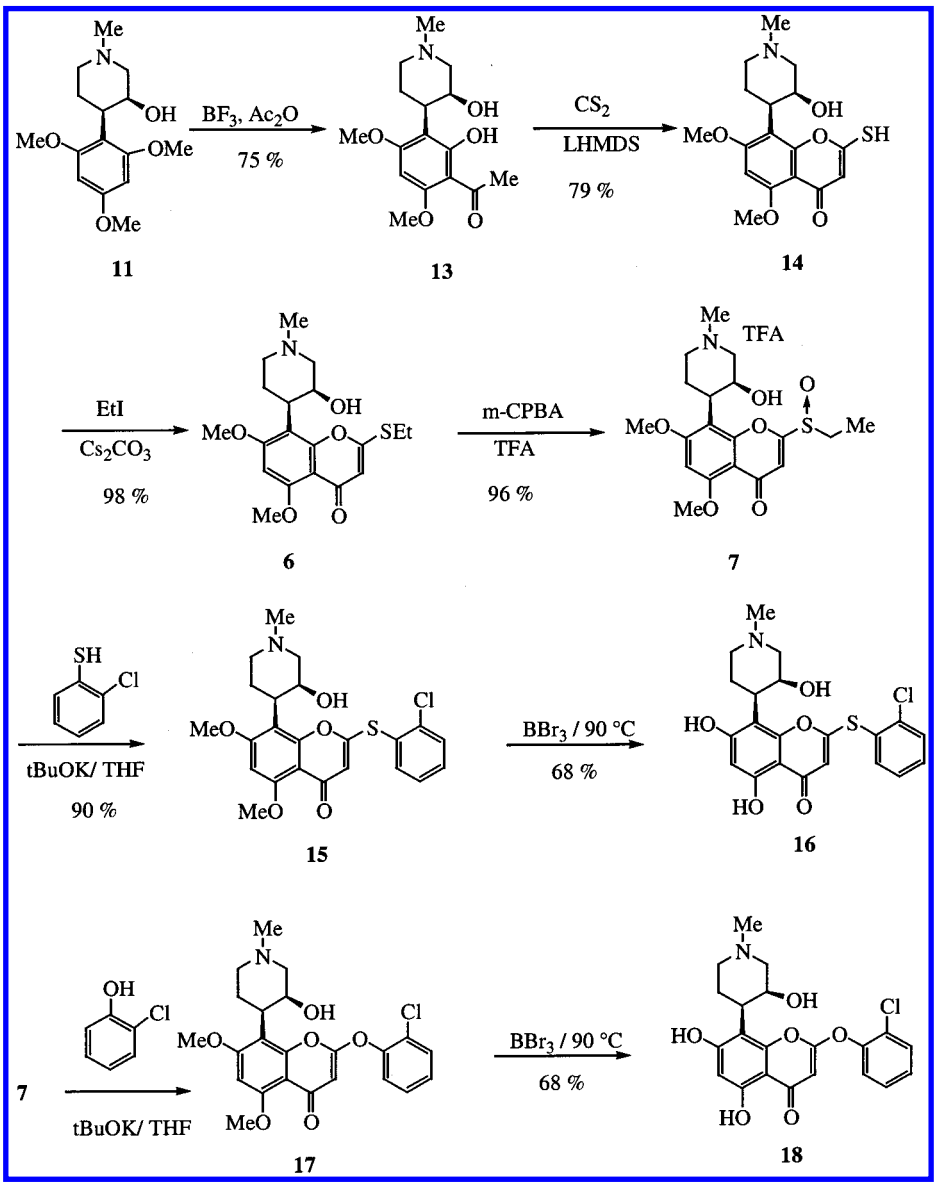

logues containing a sulfur (**16**) or oxygen (**18**) atom linker retain significant potency against CDK1 and gain selectivity within the family of CDKs (Table 1). Thio- and oxoflavopiridols **16** and **18** exhibit selectivity over CDK2 by ~20-fold and 50−150-fold over CDK4, respectively. These compounds showed competitive CDK1 inhibition with respect to ATP, and their selectivities were dependent upon the CDK subunit without being affected by the cyclin subunit (Table 2) or protein substrate (either histone H1 or Rb, data not shown). Thus far the *tert*-butyl analogue **23** is the most potent CDK1 inhibitor of the sulfur-linked series with IC_{50} = 80 nM as a racemic mixture. This compound also retains significant selectivity within the CDK family. In general, hydrophobic substituents with the sulfur or oxygen atom linker exhibit more potent CDK1/cyclin B inhibitory activity compared to the less hydrophobic analogues, and an aromatic ring is not required for good potency as seen with the *tert*-butyl analogue **23**. On the other hand, more polar substituents, **24** and **25**, significantly reduce activity against CDK1. Insertion of a nitrogen atom linker (**25**) results in a severe reduction in potency against all CDKs tested. As illustrated in Table 3, thio- and oxoflavopiridols **16** and **18** are significantly more selective for CDK1 than other CDK inhibitors described to date. In addition, each appears to retain the excellent selectivity profile of flavopiridol (**1**) when tested against unrelated serine/threonine and tyrosine protein kinases. In fact, the oxygen-linked analogue **18** is less active against PKC in comparison to flavopiridol (**1**).

The structures of flavopiridol and thioflavopiridol **16** in complex with CDK2 were determined by X-ray crystallography, revealing the molecular basis of inhibition by these molecules.[15] Figure 1a,b shows the crystal structures of flavopiridol and thioflavopiridol **16**, respectively, in the active site of CDK2 with a number of residues comprising the site. In an effort to understand the relative CDK1 selectivity of thioflavopiridol **16** over flavopiridol, an analysis of the X-ray ligand−protein contacts, a comparison of the sequences of CDK1, CDK2, and CDK4, and molecular modeling were performed. The contacts of the benzopyran ring and the piperidinyl ring of both flavopiridol and thioflavopiridol **16** with CDK2 in the X-ray structures are found to be similar to those observed by Kim et al. for deschloroflavopiri-

Scheme 3

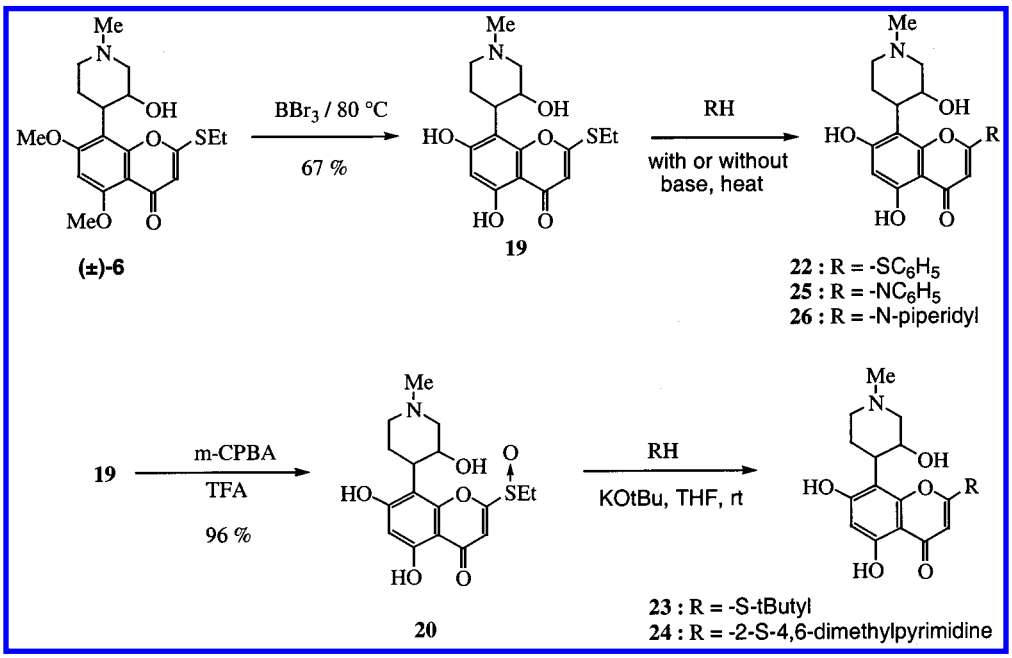

Table 1. CDK Activity Data of the Analogue

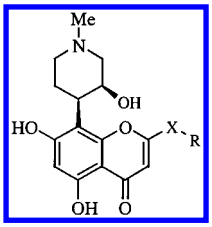

compd	X	R	IC$_{50}$ (μM) CDK1/ Cyc B1	CDK2/ Cyc E	CDK4/ Cyc D1
1, flavopiridol	none	2-chlorophenyl	0.03	0.17	0.10
19	S	ethyl (±)	0.46	3.93	2.06
16	S	2-chlorophenyl (−)	0.11	2.10	16.2
18	O	2-chlorophenyl (−)	0.13	2.11	6.15
21	S	2-chlorophenyl (+)	6.10	4.40	>25
22	S	phenyl (±)	0.44	6.59	4.10
23	S	*tert*-butyl (±)	0.08	1.07	2.07
24	S	4,6-dimethyl-pyrimidine (±)	6.40	40.4	82.5
25	NH	phenyl (±)	16.3	>25	>25
26	none	*N*-piperidyl(±)	2.50	9.69	3.70

Table 2. Activity Data of CDK Inhibitors Depending on Cyclin Subunit

compd	IC$_{50}$ (μM) CDK1/ Cyc B1	CDK1/ Cyc A	CDK2/ Cyc E	CDK2/ Cyc A
1, flavopiridol	0.03	0.05	0.17	0.07
16	0.11	0.16	5.9	1.5

dol.[16] An analysis of the sequence alignment of CDK1, CDK2, and CDK4 shows only subtle differences in the residues that comprise the buried ATP-binding site; thus selectivity is most likely due to interactions other than those deep in the ATP-binding site. An amino acid comparison of the surface-exposed hinge region and an analysis of flavopiridol and thioflavopiridol **16** docked in homology models of CDK1 and CDK4 (built from the X-ray structure of CDK2, results not published) reveal that several differences in this particular area may be playing a role in specificity (aligned sequences with

Table 3. Activity Data of CDK Inhibitors against Other Different Kinases

compd	IC$_{50}$ (μM) CDK1/ Cyc B1	CDK2/ Cyc E	CDK4/ Cyc D1	MAP	PKA	PKC	EGFR
1, flavopiridol	0.03	0.17	0.10	19.0	>50	14.0	22.0
16	0.11	2.10	16.2	>25	>50	16.1	>50
18	0.13	2.11	6.15	>25	>50	>50	>50
olomoucine	7.0	7.0	1000	30	2000	1000	440
butyrolactone I	0.60	1.50	1000	94	260	160	590

numbering from SWISS-PROT):[17] CDK1(84−89), SMDLKK; CDK2(84−89), HQDLKK; CDK4(97−102), DQDLRT.

The aforementioned differences occur in the region where the chlorophenyl ring of thioflavopiridol **16** resides and may help explain the observed selectivity. The CDK1 selectivity of thioflavopiridol **16** compared to flavopiridol is due to a relative decrease in CDK2 binding. The selectivity may result in part from a less-than-optimal interaction of thioflavopiridol **16** with Ile10, a residue conserved in CDK1, CDK2, and CDK4, coupled with a greater number of compensating interactions with CDK1 than with CDK2 or CDK4. The X-ray structure reveals that the chlorine atom of flavopiridol favorably interacts with Ile10 as a van der Waals distance of 2.99 Å to the C$^{\gamma}$ of Ile10 would indicate suggesting that this may be one of the reasons that flavopiridol increases kinase inhibition by a factor of 6 over the deschloro analogue.[18] In the CDK2 complex with thioflavopiridol **16** the side chain of Ile10 is observed to be shifted only slightly when the complex is superposed by backbone atoms with that of the flavopiridol−CDK2 complex. However, the sulfur linker of thioflavopiridol **16** places the chlorophenyl ring further away from the side chain of Ile10, relative to flavopiridol, and closer to Lys89 which is observed to be within contact distance of thioflavopiridol. The hydrocarbon portion of the side chain of Lys89 is within van der Waals contact of the chlorophenyl ring. In addition, the basic nitrogen of Lys89 adopts a geometry with respect to the chlorophenyl ring suitable for an

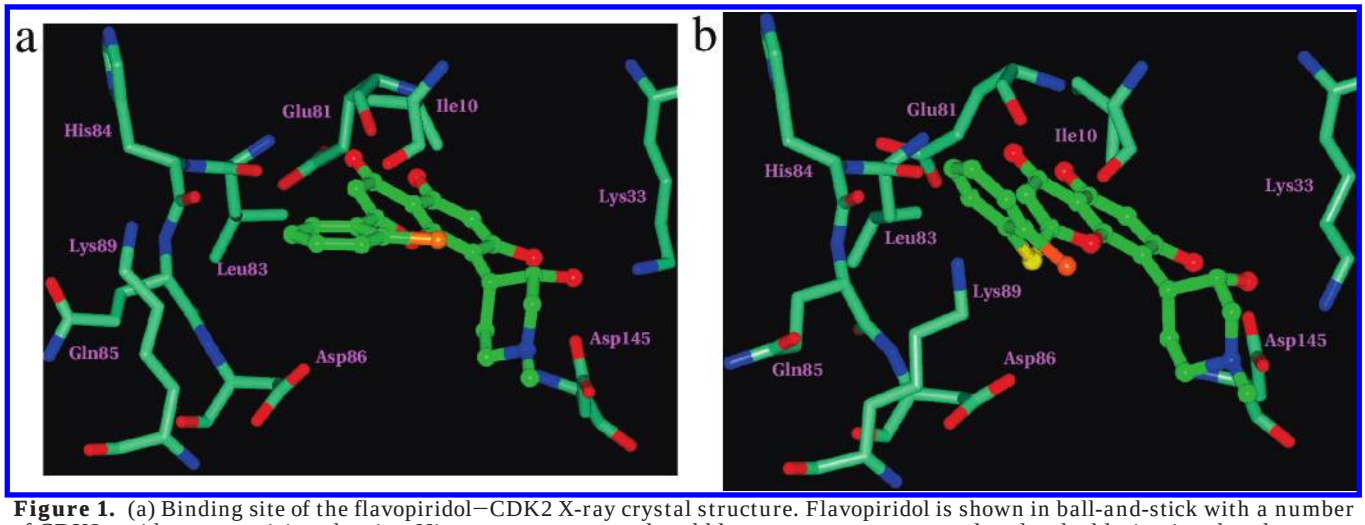

Figure 1. (a) Binding site of the flavopiridol−CDK2 X-ray crystal structure. Flavopiridol is shown in ball-and-stick with a number of CDK2 residues comprising the site. Nitrogen atoms are colored blue, oxygen atoms are colored red, chlorine is colored orange, sulfur is colored yellow, carbon atoms in thioflavopiridol are colored dark green, and carbon atoms in CDK2 are colored light green. (b) Binding site of thioflavopiridol **16**−CDK2 X-ray crystal structure. Thioflavopiridol is shown in ball-and-stick with a number of CDK2 residues comprising the site. Nitrogen atoms are colored blue, oxygen atoms are colored red, chlorine is colored orange, sulfur is colored yellow, carbon atoms in thioflavopiridol are colored dark green, and carbon atoms in CDK2 are colored light green.

Table 4. Clonogenic Assay Data

	IC_{50} (nM)			
compd	HCT116	A2780	PC3	Mia PaCa-2
1, flavopiridol	13	15	10	36
16	210	870	20	30

amino−aromatic interaction.[19] This type of interaction involving Lys89 was also observed in the crystal structure of a CDK2−olomoucine complex.[20] In the flavopiridol−CDK2 complex it is observed that Lys89 is in a different position and closer to Gln85 with a distance from the Lys side chain nitrogen to the Gln side chain oxygen of 3.59 Å. Although Lys89 is common to CDK1 and CDK2, sequence differences near this residue, e.g. Met85 (CDK1) vs Gln85 (CDK2), would not only increase the hydrophobic nature of this area but also affect packing preferences, including the conformational orientation of Lys89, such that it is steered toward the chlorophenyl ring of thioflavopiridol. CDK2/CDK4 selectivity of thioflavopiridol may be rationalized in part by the fact that the corresponding residue of Lys89 (CDK2) in CDK4 is Thr, and thus a potential favorable interaction is lost in binding to CDK4.

Thioflavopiridol **16**, the most CDK1-selective compound, was further compared to flavopiridol (**1**) in a clonogenic assay using four human tumor cell lines (Table 4). This assay demonstrated that changing the CDK selectivity profile impacted the antiproliferative activity of these small molecules. Thioflavopiridol **16** was found to be 16- and 58-fold less active than flavopiridol (**1**) when tested against HCT116 colorectal carcinoma or A2780 ovarian carcinoma cells. However, thioflavopiridol **16** is equally effective at inhibiting colony formation of PC-3 prostate carcinoma or Mia PaCa-2 pancreatic carcinoma cells. These data suggest that a CDK1-selective inhibitor may have a unique spectrum of antitumor activity and perhaps with altered or lesser side effects. Thus, thioflavopiridol **16**, a potent and more selective analogue of flavopiridol, may warrant further preclinical evaluation.

Conclusions

Enantio pure thio- and oxoflavopiridols were prepared via efficient "dynamic kinetic resolution" of intermediate piperidone **8**, and representative thio- and oxoflavopiridols **16** and **18** display CDK1 selective inhibitory activity over CDK2 by 20-fold and 50−150-fold over CDK4, respectively. These compounds do not have any appreciable inhibitory activity against other kinds of kinases such as MAP, PKA, PKC, and EGFR. It is postulated that the CDK1 selectivity of the hydrophobic group-substituted analogues containing a sulfur and oxygen linker presented in this paper is due to sequence differences in the solvent-exposed binding pocket. In a clonogenic assay using human tumor cell lines, nonselective CDK inhibitor flavopiridol and CDK1-selective thioflavopiridol **16** displayed a different spectrum of activity depending on the cell lines. We believe that these small CDK1-selective inhibitor molecules provide us with a unique opportunity to further study the biological role of CDK1/cyclin B.

Experimental Section

All new compounds were homogeneous by thin-layer chromatography and reversed-phase HPLC (>99%). Flash chromatography was carried out on E. Merck Kieselgel 60 silica gel (230−400 mesh). Preparative HPLC was run on YMC OD S-10 50- × 500-mm column eluting with a mixture of solvents A and B (starting from 10% solvent B to 100% solvent B over 30 min gradient time; solvent A: 10% MeOH−90% H_2O−0.1% TFA; solvent B: 90% MeOH−10% H_2O−0.1% TFA; flow rate: 84 mL/min; UV: 254 nm). ^1H and ^{13}C NMR spectra were obtained on a JEOL CPF-270 spectrometer operating at 270 or 67.5 MHz, respectively, and are reported as ppm downfield from an internal tetramethylsilane standard. The abbreviations of qn and sx in ^1H NMR refer to quintet and sextet, respectively. Melting points are uncorrected. Tetrahydrofuran (THF) and xylenes were dried by distillation from sodium. *N*,*N*-Dimethylformamide (DMF) was dried over 4A molecular sieves.

(*R*)-1-Methyl-4-(2,4,6-trimethoxyphenyl)-3-piperidinone (10). A mixture of (±)-1-methyl-4-(2,4,6-trimethoxyphenyl)-3-piperidinone[13] (1.60 g, 5.73 mmol) and dibenzoyl-D-tartaric acid (2.28 g, 315 mmol) in 10 mL of methanol was heated at reflux temperature until it became a homogeneous solution under argon atmosphere and it was cooled to room tempera-

ture. After stirring overnight at room temperature the precipitated solid was filtered, washed with a small amount of methanol to obtain the first crop of (*R*)-1-methyl-4-(2,4,6-trimethoxyphenyl)-3-piperidinone dibenzoyl-D-tartaric acid salt, **7** (2.65 g). The filtrate solution was concentrated to a volume of ca. 6 mL and was stirred at ambient temperature overnight. The second crop of the chiral salt (0.24 g) was obtained by filtering the solid and washing with a small amount of methanol. The combined solid salt (2.89 g) was dissolved in a mixture of CH_2Cl_2 (40 mL) and aqueous NaOH solution (12 mL of 0.5 NaOH), the organic solution was separated, washed with brine, dried over $MgSO_4$ and concentrated under reduced pressure to obtain the title compound (1.60 g, 76% yield) as a white solid: mp 131−133 °C; $[\alpha]^{25}_D$ +31° (MeOH, *c* 1.0). Optical purity of 99.9% of this enantiomer was checked by HPLC on OD Chiracel column (250 × 4.6 mm) eluting with 30% 2-propanol in hexane containing 0.1% triethylamine (flow rate: 1.0 mL/min) at 254 nm: ^{1}H NMR ($CDCl_3$) δ 6.28 (s, 2H), 4.01 (m, 1H), 3.92 (s, 3H), 3.88 (s, 6H), 3.58 (m, 1H), 3.13 (m, 1H), 2.97 (m, 1H), 2.61 (m, 1H), 2.51 (s, 3H), 2,48 (m, 1H), 2.12 (m, 1H); ^{13}C NMR ($CDCl_3$) δ 207.0, 151.5, 159.7, 109.7, 92.3, 67.7, 56.9, 56.4, 55.7, 47.2, 44.6, 30.5; MS (ESI) 446 $(M + H)^+$.

(3*S*,4*R*)-1-Methyl-4-(2,4,6-trimethoxyphenyl)-3-piperidinol (11). To a stirred solution of **10** (25.0 g, 89.5 mmol) in CH_2Cl_2 (225 mL) at −78 °C was added dropwise a solution of diisobutylaluminum hydride (180 mmol, 180 mL of 1 M solution in CH_2Cl_2) under argon atmosphere with maintaining the reaction temperature below −65 °C. The reaction mixture was stirred for 3.5 h at −78 °C after the completion of addition. Trifluoroacetic acid (50 mL) was added dropwise to the reaction mixture at −78 °C. After stirring the mixture for 15 min, MeOH (250 mL) was added. The mixture was warmed to room temperature and concentrated to obtain a solid residue, which was stirred with aqueous NaOH solution (2 N, 750 mL) for 15 min. The product was extracted with ethyl acetate (3 × 750 mL). The combined ethyl acetate solution was washed with brine, dried over Na_2SO_4 and concentrated to give a gum (25.0 g, 99%). This material was dissolved in CH_2Cl_2 and purified by flash chromatography (EtOAc:MeOH:Et_3N/100:20:0.2) to afford a mixture of *cis*- and *trans*-alcohols as a foam (22.0 g). This isomeric mixture was dissolved in 30% 2-propanol in hexanes and passed through a Chiracel AD column (50 × 50 mm; Daicel Chem. Ind. Ltd.) eluting with 30% 2-propanol in hexanes containing 0.2% Et_3N to obtain the title compound as a pure *cis*-alcohol **11** (14.1 g, 56%): mp 111−112 °C (lit.[13] 109−111 °C); $[\alpha]^{25}_D$ −53.8° (MeOH, *c* 1.0) (lit.[13] −54.13°); ^{1}H NMR ($CDCl_3$) δ 6.13 (s, 2H), 3.82 (m, 1H), 3.82 (s, 9H), 3.32 (m, 1H), 3.00 (m, 2H), 2.87 (m, 1H), 2.30 (s, 3 H), 2.10 (m, 3H), 1.40 (m, 1H); ^{13}C NMR ($CDCl_3$) δ159.6, 159.2, 111.5, 91.5, 70.4, 62.6, 57.1, 55.8, 55.3, 46.4, 36.8, 24.3.

(3*S*,4*R*)-4-(3-Acetyl-2-hydroxy-4,6-dimethoxyphenyl)-1-methyl-3-piperidinol (13). A solution of **11** (13.8 g, 49 mmol) in CH_2Cl_2 (250 mL) at 0 °C was added BF_3 etherate (50 mL) followed by acetic anhydride (40 mL). The resulting mixture was stirred at room temperature overnight and concentrated. The residue was cooled in an ice bath and quenched with MeOH (300 mL) and the mixture was stirred at room temperature for 15 min and concentrated in vacuo. The residue was dissolved in MeOH (300 mL) and stirred with 20% aqueous KOH solution (200 mL) for 48 h. It was mostly concentrated and pH of the residue was adjusted to 9.5 with 4 N hydrochloric acid. The product was extracted with CH_2Cl_2 (5 × 100 mL) and the combined CH_2Cl_2 extracts was dried over Na_2SO_4 and concentrated to afford a solid. This solid was purified by flash column chromatography (EtOAc:MeOH:Et_3N/100:15:0.2) to obtain a pure product which was triturated with diisopropyl ether (150 mL) to give **13** (12.5 g, 82.6%) as a light yellow solid: mp 182 °C (lit.[13] 184−186 °C); $[\alpha]^{25}_D$ −34.5° (MeOH, *c* 1.0) (lit.[13] −32.65°); ^{1}H NMR ($CDCl_3$) δ 14.40 (s, 1H), 6.11 (s, 1H), 4.51 (s, broad, 1H), 4.03 (s, 3H), 4.01 (s, 3H), 4.0 (s, 1H), 3.50 (m, 1H), 3.16 (m, 3H), 2.73 (s, 3H), 2.46 (s, 3H). 2.36 (m, 1H), 2.22 (m, 1H), 1.56 (m, 1H); ^{13}C NMR ($CDCl_3$) δ 203.3, 264.0, 163.7, 161.7, 109.9, 105.6, 86.1, 69.8, 62.2, 56.6, 55.2, 55.0, 46.0, 36.4, 32.8, 23.7; MS (ESI) 310 $(M + H)^+$.

(3*S*,4*R*)-2-(Ethylthio)-8-(3-hydroxy-1-methyl-4-piperidyl)-5,7-dimethoxy-4*H*-1-benzopyran-4-one (6). To a suspension of **13** (6.5 g, 21.01 mmol) in anhydrous THF (85 mL) under argon was added carbon disulfide (7 mL). The slurry was cooled to 0 °C (ice bath) and lithium bis(trimethylsilyl)amide (1.0 M solution in THF, 126 mL) was slowly added at such a rate that the temperature of the slurry was maintained below 18 °C. After the addition was complete, the solution was gradually warmed to room temperature and stirred for 2 h. Water (50 mL) was added to the mixture, stirred and concentrated in vacuo. The residue was cooled to 0 °C, methanol (80 mL) was added followed by 50% aqueous trifluoroacetic acid (30 mL). After stirring at room temperature for 1.0 h. the solution was concentrated in vacuo. The residue was triturated with a small amount of ethyl acetate and the solid was filtered to obtain crude thiol **14** (6.5 g). This crude thiol compound was used directly for the next step without further purification.

To a stirred solution of crude thiol **14** (6.5 g, 21.01 mmol) at 0 °C in anhydrous DMF (75 mL) under argon was added cesium carbonate (35 g). The resulting suspension was stirred at 0 °C for 30 min, then iodoethane (1.75 mL) was added. The mixture was stirred at 0 °C for 1 h and then at room temperature for 18 h. The reaction mixture was diluted with water (300 mL) and the product was extracted with dichloromethane (3 × 300 mL). The combined dichloromethane extracts was washed with 10% aqueous lithium chloride, water and brine, dried over anhydrous Na_2SO_4 and concentrated in vacuo to give crude **6** as a gum (5.0 g). The crude material was purified by flash chromatography (ethyl acetate−methanol−triethylamine/10:0.5:0.2 and 10:1:0.2) to give 3.81 g of pure **6** (50%) as a solid: $[\alpha]^{25}_D$ −74.0° (MeOH, *c* 0.42); ^{1}H NMR ($CDCl_3$) δ 1.43 (t, J = 7.6 Hz, 3H), 1.58 (m, 1H), 2.05 (m, 1H), 2.23 (m, 1H), 2.35 (s, 3H), 3.02 (m, 5H), 3.26 (s, broad, 1H), 3.35 (m, 1H), 3.86 (m, 1H), 3.94 (s, 3H), 3.97 (s, 3H), 6.43 (s, 1H), 6.46 (s, 1H); ^{13}C NMR ($CDCl_3$) δ 157.8, 165.1, 162.1, 159.7, 157.6, 110.3, 109.9, 108.8, 92.5, 69.9, 62.8, 57.1, 56.4, 56.0, 46.4, 38.4. 25.5, 24.5, 14.2; MS (ESI) 380 $(M + H)^+$. Anal. ($C_{19}H_{25}NO_5S\cdot0.25H_2O$) C, H, N, S.

(3*S*,4*R*)-2-(Ethylsulfinyl)-8-(3-hydroxy-1-methyl-4-piperidinyl)-5,7-dimethoxy-4*H*-1-benzopyran-4-one, Trifluoroacetic Acid Salt (7). To a solution of **6** (1.67 g, 4.41 mmol) in CH_2Cl_2 (18 mL) containing TFA (1.7 mL) at 0 °C was added *m*-chloroperbenzoic acid (1.42 g, 50−60% contents) as a solid with stirring. The mixture was stirred at 0 °C for 1 h and then quenched by adding dimethyl sulfide (1 mL). The mixture was stirred for 5 min and concentrated in vacuo. To the residue was added ethyl ether (150 mL) and the mixture was stirred at room temperature for 30 min. The precipitated solid was filtered and dried to obtain the sulfoxide **7** (2.15 g) as a diastereomeric mixture, which was contaminated by a very small amount of overoxidized sulfone product. This crude diastereomeric mixture was used for the next reaction without any further purification: ^{1}H NMR (CD_3OD) δ 6.66 (s, 1H), 6.62(s, 1H), 6.34 (s, 1H), 6.32 (s, 1H), 4.21 (s, 1H), 4.15 (s, 1H), 3.66−3.04 (m, 8H), 2.91 (s, 3H), 1.88 (m, 1H), 1.32 (t, J = 7.3 Hz, 3H), 1.26 (t, J = 7.3 Hz, 3H); ^{13}C NMR (CD_3OD) δ 182.3, 182.2, 171.0, 169.8, 165.0, 164.7, 162.8, 158.4 158.1, 110.4, 109.6, 107.6, 107.5, 106.4, 106.2, 101.4, 100.9, 67.8, 67.7, 61.9, 61.7, 56.8, 56.7, 47.4, 46.6, 44.4, 44.3, 37.5, 37.3, 23.5, 6.1, 5.2; MS (ESI) 396 $(M + H)^+$.

(3*S*,4*R*)-2-[(2-Chlorophenyl)thio]-8-(3-hydroxy-1-methyl-4-piperidinyl)-5,7-dimethoxy-4*H*-1-benzopyran-4-one (15). A mixture of potassium *tert*-butoxide (1.12 g, 10 mmol) and 2-chlorothiophenol (1.16 g, 8 mmol) in THF (10 mL) was stirred at room temperature under argon atmosphere for 10 min. To this mixture at 0 °C was added a solution of **7** (1.0 g, 1.96 mmol) in THF (10 mL). The resulting mixture was stirred at 0 °C for 1 h and it was directly loaded onto a chromatography column (SiO_2) and eluted with ethyl acetate (ca. 1 L) followed by EtOAc:MeOH:Et_3N (100:15:2) to afford the desired product. This material was dissolved in CH_2Cl_2 (100 mL), washed with aqueous $NaHCO_3$ solution, dried over Na_2SO_4 and concentrated in vacuo to afford **15** (830 mg, 92%)

as a solid: mp 185−187 °C; $[\alpha]^{25}_D$ −59.8° (MeOH, *c* 0.41); ^{1}H NMR (CD_3OD) δ 1.54 (m, 1H), 2.33 (m, 2H), 2.48 (s, 3H), 3.08 (m, 4H), 3.70 (m, 1H), 3.96 (s, 3H), 3.98 (s, 3H), 4.60 (s, 1H), 6.00 (s, 1H), 6.63 (s, 1H),7.47 (m, 1H), 7.58 (m, 1H), 7.66 (d, J = 8.2 Hz, 1H), 7.80 (d, J = 6.6 Hz, 1H); ^{13}C NMR (CD_3OD) δ 179.3, 166.2, 165.9, 162.4, 160.3, 140.8, 139.1, 134.6, 133.3, 130.9, 129.1, 113.0, 111.6, 109.8, 95.5, 70.5, 63.8, 58.6, 57.9, 57.8, 46.8, 40.3, 25.7; MS (ESI) 462 $(M + H)^+$.

(3*S*,4*R*)-2-[(2-Chlorophenyl)thio]-5,7-dihydroxy-8-(3-hydroxy-1-methyl-4-piperidinyl)-4*H*-1-benzopyran-4-one (16). To a stirred solution of **15** (2.6 g, 5.63 mmol) in 1,2-dichloroethane (50 mL) under argon was slowly added boron tribromide (2.0 M solution in 1,2-dichloroethane, 28 mL). After the addition was complete, the suspension was heated at 85−90 °C for 4 h. The mixture was cooled and then concentrated in vacuo. To the residue at −30 °C (dry ice−acetonitrile bath) methanol (50 mL) was slowly added and the solution was gradually warmed to room temperature. Sodium bicarbonate (8 g) was added as a solid, stirred for 30 min and the mixture was acidified with trifluoroacetic acid to pH 2.0. The mixture was concentrated in vacuo to give a semisolid product (1.69 g). This material was purified by preparative HPLC to obtain the product as a trifluoroacetic acid salt. The trifluoroacetate salt was dissolved in methanol (70 mL) containing aqueous 1 N hydrochloric acid (15 mL), concentrated in vacuo to a small volume and then lyophilized to give 1.94 g (69%) of the HCl salt of **16** as a light yellow powder: mp 110 °C; $[\alpha]^{25}_D$ −7.1° (MeOH, *c* 0.32); ^{1}H NMR (CD_3OD) δ 1.66 (m, 1H), 2.90 (s, 3H), 3.50−2.91 (m, 7H), 4.05 (m, 1H), 5.93 (s, 1H), 6.29 (s, 1H), 7.87−7.50 (m, 4H); ^{13}C NMR (CD_3OD) δ 182.2, 168.7, 164.3, 162.2, 157.9, 140.3, 138.8, 133.9, 132.3, 129.9, 127.4, 108.3, 106.8, 105.2, 101.4, 67.8, 61.7, 56.8, 44.4, 37.1, 23.1; MS (ESI) 434 $(M + H)^+$. Anal. ($C_{21}H_{20}NO_5SCl\cdot HCl\cdot 1.1H_2O$) C, H, N, S, Cl.

(3*S*,4*R*)-2-(2-Chlorophenoxy)-8-(3-hydroxy-1-methyl-4-piperidinyl)-5,7-dimethoxy-4*H*-1-benzopyran-4-one (17). A mixture of 2-chlorophenol (1.0 mL, 9.65 mmol) and potassium *tert*-butoxide (1.20 g, 10.69 mmol) in anhydrous THF (12 mL) was stirred for 10 min at room temperature, then cooled in an ice bath and sulfoxide **7** (1.15 g, 2.26 mmol) was added. The reaction mixture was stirred at 0−5 °C for 1.5 h. After adding acetic acid (0.25 mL) to the mixture it was directly loaded onto a silica gel column and eluted with ethyl acetate followed by EtOAc:MeOH:Et_3N (100:20:2) to obtain after concentration a product containing trifluoroacetic acid and triethylamine. This material was mixed with chloroform (60 mL) and aqueous $NaHCO_3$ (10 mL) solution, the organic layer was separated, dried over magnesium sulfate and concentrated in vacuo to obtain **17** (760 mg, 76%) as a floppy glassy material: $[\alpha]^{25}_D$ −55.6° (MeOH, *c* 0.7); ^{1}H NMR ($CDCl_3$) δ 7.54 (dd, J = 7.0, 2.3 Hz, 1H), 7.40−7.34 (m, 3H), 6.44 (s, 1H), 5.39 (s, 1H), 3.96 (s, 3H), 3.93 (s, 3H), 3.74 (s, broad, 1H), 3.19−2.85 (m, 6H), 2.28 (s, 3H), 1.85−2.05 (m, 1H), 1.48−1.60 (m, 1H); ^{13}C NMR ($CDCl_3$) δ 179.4, 164.1, 162.2, 159.9, 155.1, 147.8, 131.8, 128.7, 128.1, 127.3, 123.4, 111.0, 108.2, 93.2, 91.1, 70.1, 62.8, 57.1, 56.7, 56.3, 46.7, 46.4, 38.4, 24.8; MS (ESI) 446 $(M + H)^+$.

(3*S*,4*R*)-2-(2-Chlorophenoxy)-5,7-dihydroxy-8-(3-hydroxy-1-methyl-4-piperidinyl)-4*H*-1-benzopyran-4-one (18). To a solution of **17** (760 mg, 1.70 mmol) in 1,2-dichloroethane (20 mL) at room temperature was added a solution of boron tribromide (8.5 mL of 2 M solution in 1,2-dichloroethane, 17.0 mmol). The mixture was stirred at 80 °C for 5 h, cooled and concentrated in vacuo. To the residue at −30 °C methanol (10 mL) was added followed by solid $NaHCO_3$ (1.5 g) and it was stirred at room temperature for 10 min. After acidifying the mixture with TFA (0.5 mL) it was concentrated to a small volume and the residue was purified by preparative HPLC to obtain the trifluoroacetic acid salt of **18** (505 mg, 53%) as a solid: mp 105 °C (softened); $[\alpha]^{25}_D$ −22.4° (MeOH, *c* 0.7); ^{1}H NMR (CD_3OD) δ 7.65 (d, J = 8.2 Hz, 1H), 7.48 (m, 3H), 6.30 (s, 1H), 5.20 (s, 1H), 4.20 (m, 1H), 3.51 (m, 3H), 3.18 (m, 3H), 2.87 (s, 3H), 1.80 (m, 1H); ^{13}C NMR (CD_3OD) δ 186.5, 168.5, 164.8, 162.8, 155.8, 149.2, 133.3, 131.2, 130.8, 128.4, 125.3, 107.8, 104.8, 102.1, 89.1, 68.6, 62.5, 57.6, 45.0, 38.2, 24.0; MS (ESI) 418 $(M + H)^+$. Anal. ($C_{21}H_{20}ClNO_6\cdot 0.5H_2O\cdot 1.15CF_3COOH$) C, H, N, F, Cl.

(±)-(3*SR*,4*RS*)-2-(Ethylthio)-5,7-dihydroxy-8-(3-hydroxy-1-methyl-4-piperidinyl)-4*H*-1-benzopyran-4-one (19). To a solution of racemic **6** (144 mg, 0.4 mmol) in 1,2-dichloroethane (2 mL) at room temperature was added a solution of boron tribromide (800 mg, 3.2 mmol). The mixture was stirred at 80 °C for 5 h, cooled to 0 °C, quenched by methanol (5 mL), and it was neutralized by aqueous $NaHCO_3$ solution. After concentrating in vacuo the residue was purified by preparative HPLC to obtain the trifluoroacetic acid salt of **19** (121 mg, 67%) as a solid: mp 105−107 °C; ^{1}H NMR (CD_3OD) δ 6.27 (s, 1H), 6.15 (s, 1H), 4.24 (s, 1H), 3.63−3.12 (m, 8H), 2.90 (s, 3H), 1.85 (m, 1H), 1.42 (t, J = 7.6 Hz, 3H); ^{13}C NMR (CD_3OD) δ 182.0, 171.7, 163.9, 162.2, 158.1, 106.9, 106.7, 105.2, 101.0, 68.0, 61.8, 56.8, 44.2, 37.4, 26.6, 23.3, 14.3; MS (ESI) 352 $(M + H)^+$. Anal. ($C_{17}H_{21}NO_5S\cdot 1.0H_2O\cdot 1.1CF_3COOH$) C, H, N.

(±)-(3*SR*,4*RS*)-2-(Ethylsulfinyl)-8-(3-hydroxy-1-methyl-4-piperidinyl)-5,7-dihydroxy-4*H*-1-benzopyran-4-one, Trifluoroacetic Acid Salt (20). To a solution of **19** (0.99 g, 2.0 mmol) in CH_2Cl_2 (20 mL) containing TFA (0.8 mL) at 0 °C was added *m*-chloroperbenzoic acid (0.576 g, 50−60% contents) as a solid with stirring. The mixture was stirred at 0 °C for 2 h and then quenched by adding dimethyl sulfide (0.15 mL). The mixture was stirred for 5 min and concentrated in vacuo. To the residue was added ethyl ether (150 mL) and the mixture was stirred at room temperature for 30 min. The precipitated solid was filtered and dried to obtain the trifluoroacetic acid salt of sulfoxide **20** (0.955 g, 96%) as a diastereomeric mixture, which was contaminated by a very small amount of overoxidized sulfone product. This crude diastereomeric mixture was used for the next reaction without any further purification: ^{1}H NMR (CD_3OD) δ 6.66 and 6.62 (s, ea, 1H), 6.34 and 6.32 (s, ea, 1H), 4.21 and 4.15 (m, 1H), 3.66−3.04 (m, 8H), 2.91 (s, 3H), 1.88 (m, 1H), 1.32 and 1.26 (t, ea, J = 7.3 Hz, 3H); ^{13}C NMR (CD_3OD) δ 182.3 and 182.2, 171.0, 169.8, 165.0, 164.7, 162.8, 158.4 and 158.1, 110.4, 109.6, 107.6 and 107.5, 106.4 and 106.2, 101.4, 100.9, 67.8 and 67.7, 61.9 and 61.7, 56.8 and 56.7, 47.4, 46.6, 44.4 and 44.3, 37.5 and 37.3, 23.5, 6.1, 5.2.

(±)-(3*SR*,4*RS*)-2-(Phenylthio)-5,7-dihydroxy-8-(3-hydroxy-1-methyl-4-piperidinyl)-4*H*-1-benzopyran-4-one (22). A mixture of **19** (50 mg, 0.1 mmol), thiophenol and $NaHCO_3$ (100 mg) in DMF (0.5 mL) was stirred at 100 °C for 2 h, cooled to room temperature and the solid was filtered off. The filtrate solution was purified by preparative HPLC to obtain the trifluoroacetic acid salt of **22** (21 mg, 35%) as a solid: mp 82−84 °C; ^{1}H NMR (CD_3OD) δ 7.73−7.59 (m, 5H), 6.25 (s, 1H), 5.86 (s, 1H), 4.08 (s, 1H), 3.52−2.93 (m, 6H), 2.88 (s, 3H), 1.68 (m, 1H); ^{13}C NMR (CD_3OD) δ 182.1, 171.0, 164.1, 162.1, 157.9, 136.6, 132.0, 131.5, 128.0, 107.7, 106.7, 105.1, 101.3, 67.8, 61.7, 56.7, 44.3, 37.1, 23.1; MS (ESI) 400 $(M + H)^+$. Anal. ($C_{21}H_{21}NO_5S\cdot 0.5H_2O\cdot 1.6CF_3COOH$) C, H, N.

(±)-(3*SR*,4*RS*)-2-(*tert*-Butylthio)-5,7-dihydroxy-8-(3-hydroxy-1-methyl-4-piperidinyl)-4*H*-1-benzopyran-4-one (23). A mixture of sulfoxide **20** (50 mg, 0.1 mmol), *tert*-butylthiol (45 mg, 0.5 mmol) and KOtBu (56 mg, 0.5 mmol) in THF (1.5 mL) was stirred at room temperature for 0.5 h. Trifluoroacetic acid (20 μL) was added to the reaction mixture, and it was purified by preparative HPLC to obtain the trifluoroacetic acid salt of **23** (32 mg, 84%) as a solid: mp 70−72 °C; ^{1}H NMR (CD_3OD) δ 6.48 (s, 1H), 6.30 (s, 1H), 4.25 (s, 1H), 3.70−3.47 (m, 3H), 3.34−3.15 (m, 3H), 2.91 (s, 3H), 1.82 (m, 1H), 1.53 (s, 9H); MS (ESI) 380 $(M + H)^+$; HRMS FAB $(M + H)^+$ calcd for $C_{19}H_{25}NO_5S$ 380.1532, found 380.1541.

(±)-(3*SR*,4*RS*)-2-[(4,6-Dimethylpyrimidin-2-yl)thio]-5,7-dihydroxy-8-(3-hydroxy-1-methyl-4-piperidinyl)-4*H*-1-benzopyran-4-one (24). A mixture of sulfoxide **20** (50 mg, 0.1 mmol), 4,6-dimethyl-2-mercaptopyrimidine (56 mg, 0.4 mmol) and KOtBu (45 mg, 0.4 mmol) in THF (1.0 mL) was stirred at room temperature for 2 h. Trifluoroacetic acid (20 μL) was added to the reaction mixture, and it was purified by preparative HPLC to obtain the trifluoroacetic acid salt of **24** (33 mg, 76%) as a solid: mp 93−95 °C; ^{1}H NMR (CD_3OD) δ 7.08 (s, 1H), 6.76 (s, 1H), 6.33 (s, 1H), 4.16 (s, 1H), 3.56−3.04

Table 5. Summary of the Crystallographic Data Collection, Reduction, and Refinement

	flavopiridol	thioflavopiridol **16**
space group	$P2_12_12_1$	$P2_12_12_1$
real space cell parameters:		
a (Å^2)	53.27	52.99
b (Å^2)	71.67	70.76
c (Å^2)	72.38	71.87
number of observations	42445	74340
number of unique reflections	13272	17687
R_{symm} (on *R*) (%)	7.76	9.55
max observed resolution (Å^2)	2.2	1.9
completeness (%)	85.3	74.1
crystallographic *R*-factor (%)	23.7	28.0
average *B*-factor (protein) (Å^2)	22.46	20.98
average *B*-factor (ligand) (Å^2)	35.37	52.46
residues in final model	298	298
total number of atoms	2426	2427
rms (bonds) (Å^2)	0.014	0.014
rms (angles) (deg)	1.936	1.948
rms (impropers) (deg)	1.810	1.696

(m, 6H), 2.80 (s, 3H), 2.40 (s, 6H), 1.70 (m, 1H); MS (ESI) 430 $(M + H)^+$. Anal. ($C_{21}H_{23}N_3O_5S \cdot 1.0H_2O \cdot 1.3CF_3COOH$) C, H, N, F, S.

(±)-(3*SR*,4*RS*)-2-(Phenylamino)-5,7-dihydroxy-8-(3-hydroxy-1-methyl-4-piperidinyl)-4*H*-1-benzopyran-4-one (25). A mixture of **19** (50 mg, 0.1 mmol) and aniline (0.1 mL) was stirred at 120 °C for 16 h, cooled to room temperature and it was purified by preparative HPLC to obtain the trifluoroacetic acid salt of **25** (26 mg, 46%) as a solid: mp 243−245 °C dec; ^{1}H NMR (CD_3OD) δ 7.46−7.23 (m, 5H), 6.35 (s, 1H), 5.44 (s, 1H), 4.26 (s, 1H), 3.90−3.06 (m, 6H), 2.90 (s, 3H), 1.76 (m, 1H); ^{13}C NMR (CD_3OD) δ 183.4, 164.5, 163.2, 161.3, 155.9, 138.5, 131.0, 127.1, 124.3, 112.0, 103.7, 95.8, 68.9, 62.1, 57.1, 44.5, 36.5, 23.3; MS (ESI) 383 $(M + H)^+$. Anal. ($C_{21}H_{22}N_2O_5 \cdot 0.5H_2O \cdot 1.5CF_3COOH$) C, H, N.

(±)-(3*SR*,4*RS*)-2-*N*-Piperidyl-5,7-dihydroxy-8-(3-hydroxy-1-methyl-4-piperidinyl)-4*H*-1-benzopyran-4-one (26). A mixture of **19** (50 mg, 0.1 mmol) and piperidine (0.1 mL) was stirred at 120 °C for 2 h, cooled to room temperature and it was purified by preparative HPLC to obtain the trifluoroacetic acid salt of **26** (42 mg, 68%) as a solid: mp 81−83 °C; ^{1}H NMR (CD_3OD) δ 6.20 (s, 1H), 4.90 (s, 1H), 4.25 (s, 1H), 3.61−3.18 (m, 10H), 2.92 (s, 3H), 1.85−1.74 (m, 7H); ^{13}C NMR (CD_3OD) δ 183.0, 164.4, 162.9, 162.0, 155.1, 106.6, 103.4, 101.0, 68.5, 62.2, 57.0, 48.1, 44.6, 37.9, 26.7, 25.4, 23.6; MS (ESI) 375 $(M + H)^+$. Anal. ($C_{20}H_{26}N_2O_5 \cdot 0.75H_2O \cdot 2.0CF_3COOH$) C, H, N.

Crystal Structure of Human CDK2. Crystals of CDK2 were grown at room temperature by the hanging drop vapor diffusion method using 35% poly(ethylene glycol) 5000 monomethyl ester, 0.2 M ammonium acetate, 0.1 M HEPES, pH 7.0, as a reservoir solution. The hanging drop consisted of 10λ of the concentrated protein mixed with an equal volume of reservoir solution. Prior to data collection, crystals were transferred to a vial containing the mother liquor with 2.4−3.0 nM ligand added and allowed to soak for 3 days. For X-ray crystallographic data collection, the crystal was transferred to a vial containing the mother liquor with 15% glycerol added. The crystal was then flash cooled by transferring the crystal on a nylon loop to a stream of liquid nitrogen at 100 K for data collection. Data were collected on a Siemens Hi-Star area detector system using mirror focused Cu Kα radiation from a Rigaku RU-2000 rotating anode. The X-ray intensity data was reduced using program XENGEN[21] and refined by the method of simulated annealing using program XPLOR.[22] Details of the data collection and reduction are listed in Table 5.

CDK1/Cyclin B1 Kinase Assay. Kinase reactions consisted of 100 ng of baculovirus expressed GST-CDK1/cyclin B1 (human) complex, 1 μg histone HI (Boehringer Mannheim, Indianapolis, IN), 0.2 μCi [γ-^{33}P]ATP, 25 μM ATP in 50 μL kinase buffer (50 mM Tris, pH 8.0, 10 mM $MgCl_2$, 1 mM EGTA, 0.5 mM DTT). Reactions were incubated for 45 min at 30 °C and stopped by the addition of cold trichloroacetic acid (TCA) to a final concentration 15%. TCA precipitates were collected onto GF/C unifilter plates (Packard Instrument Co., Meriden, CT) using a Filtermate universal harvester (Packard Instrument Co., Meriden, CT) and the filters were quantitated using a TopCount 96-well liquid scintillation counter (Packard Instrument Co., Meriden, CT). Dose−response curves were generated to determine the concentration required to inhibit 50% of kinase activity (IC_{50}). Compounds were dissolved at 10 mM in dimethylformamide (DMF) and evaluated at six concentrations, each in triplicate. The final concentration of DMF in the assay equaled 2%. IC_{50} values were derived by nonlinear regression analysis and have a coefficient of variance (SD/mean, $n = 6$) = 16%.

CDK2/Cyclin E Kinase Assay. Kinase reactions consisted of 5 ng of baculovirus expressed GST-CDK2/cyclin E (human) complex, 0.5 μg GST-RB fusion protein (amino acids 776−928 of retinoblastoma protein), 0.2 μCi [γ-^{33}P]ATP, 25 μM ATP in 50 μL kinase buffer (50 mM Hepes, pH 8.0, 10 mM $MgCl_2$, 1 mM EGTA, 2 mM DTT). Reactions were incubated for 45 min at 30 °C and stopped by the addition of cold trichloroacetic acid (TCA) to a final concentration 15%. TCA precipitates were collected onto GF/C unifilter plates (Packard Instrument Co., Meriden, CT) using a Filtermate universal harvester (Packard Instrument Co., Meriden, CT) and the filters were quantitated using a TopCount 96-well liquid scintillation counter (Packard Instrument Co., Meriden, CT). Dose−response curves were generated to determine the concentration required inhibiting 50% of kinase activity (IC_{50}). Compounds were dissolved at 10 mM in DMF and evaluated at six concentrations, each in triplicate. The final concentration of DMF in the assay equaled 2%. IC_{50} values were derived by nonlinear regression analysis and have a coefficient of variance (SD/mean, $n = 6$) = 14%.

CDK4/Cyclin D1 Kinase Assay. Kinase reactions consisted of 150 ng of baculovirus expressed GST-CDK4/cyclin D1 (human), 280 ng of Stag-cyclin D1, 0.5 μg GST-RB fusion protein (amino acids 776−928 of retinoblastoma protein), 0.2 μCi [γ-^{33}P]ATP, 25 μM ATP in 50 μL kinase buffer (50 mM Hepes, pH 8.0, 10 mM $MgCl_2$, 1 mM EGTA, 2 mM DTT). Reactions were incubated for 1 h at 30 °C and stopped by the addition of cold trichloroacetic acid (TCA) to a final concentration 15%. TCA precipitates were collected onto GF/C unifilter plates (Packard Instrument Co., Meriden, CT) using a Filtermate universal harvester (Packard Instrument Co., Meriden, CT) and the filters were quantitated using a TopCount 96-well liquid scintillation counter (Packard Instrument Co., Meriden, CT). Dose−response curves were generated to determine the concentration required inhibiting 50% of kinase activity (IC_{50}). Compounds were dissolved at 10 mM in DMF and evaluated at six concentrations, each in triplicate. The final concentration of DMF in the assay equaled 2%. IC_{50} values were derived by nonlinear regression analysis and have a coeficient of variance (SD/mean, $n = 6$) =18%.

Kinase assays for PKA and EGFR were carried out using a TCA precipitation procedure identical to those described earlier. PKA (2 units) from bovine heart (Sigma Chemical Co.) was reacted with 500 ng of GST-TK fusion protein substrate (generated using pGEX-2TK expression construct, Pharmacia) for 1 h at 30 °C in 50 mM Tris pH 7.5, 10 mM $MgCl_2$ and 25 μM [γ-^{32}P]ATP. EGFR (50 ng catalytic domain produced in baculovirus infected Sf9 cells as a GST-fusion protein) was reacted with 1 μg poly(Glu-Tyr) for 1 h at 30 °C in 50 mM Tris pH 7.5, 10 mM $MgCl_2$, 2 mM $MnCl_2$ and 25 μM [γ-^{32}P]ATP.

The MAP kinase and PKC reactions were quantitated by spotting onto p81 phosphocellulose as described for the PKC assay system from Gibco BRL. MAP kinase p42, of xenopus origin (Santa Cruz Biotechnology Inc.), was reacted with 1 mM substrate peptide (APRTPGGRR) for 1 h at 30 °C in 50 mM Tris pH 8.0, 10 mM $MgCl_2$, 0.5 mM EGTA, 1mM DTT and 25 μM [γ-^{32}P]ATP. PKC was assayed using the PKC assay system from Gibco BRL at an ATP concentration of 20 μM. PKC (mixture of α, β and γ isoforms from rat brain) was purchased from Upstate Biotechnology.

Clonogenic Assay. Colony growth inhibition was measured for four human tumor cell lines (HCT116 colorectal carcinoma, A2780 ovarian carcinoma, A549 lung carcinoma and Mia PaCa-2 pancreatic carcinoma) using a standard clonogenic

assay. Briefly, 200 cells/well were seeded into 6-well tissue culture plates (Falcon, Franklin Lakes, NJ) and allowed to attach for 18 h. Assay medium consisted of either McCoy's 5a, RPMI-1640, Ham's F12K or DMEM plus 10% fetal bovine serum for the HCT116, A2780, A549 and Mia PaCa-2 cell lines, respectively. Cells were then treated in duplicate with a six concentration dose−response curve. The maximum concentration of DMF never exceeded 0.25%. Compound was replaced and the colonies were fed with fresh media every third day. Colony number was scored on day 10 using a BioTran III colony counter (New Brunswick Scientific Co., Edison, NJ). The compound concentration required to inhibit 50% of colony formation (IC_{50}) was determined by nonlinear regression analysis. The coefficient of variance (SD/mean, $n = 3$) = 30%.

Acknowledgment. Microanalysis and mass spectra were kindly provided by the Bristol-Myers Squibb Department of Analysis Research and Development. CDK2-expressing baculovirus and purification procedures were provided by Nikola P. Pavletich, Memorial Sloan-Kettering Cancer Center, New York.

References

(1) (a) Hunter, T.; Pines, J. Cyclins and Cancer II. Cyclin and CDK inhibitors come of age. *Cell* **1994**, *79*, 573−582. (b) Sherr, C. Cancer cell cycles. *Science* (*Washington, DC*) **1996**, *274*, 1672−1677.

(2) A review article: Pines, J. The cell cycle kinases. *Semin. Cancer Biol.* **1994**, *5*, 305−313.

(3) (a) Nigg, E. A. Cellular substrates of p34cdc2 and its companion cyclin-dependent kinases. *Trends Cell Biol.* **1993**, *3*, 296−301. (b) Rickert P.; Seghezzi, W.; Shanahan, F.; Cho, H.; Lees, E. Cyclin C/CDK8 is a novel CTD kinase associated with RNA polymerase II. *Oncogene* **1996**, *12*, 2631−2640. (c) Dynlacht, B. D.; Moberg, K.; Lees, J. A.; Harlow, E.; Zhu, L. Specific regulation of E2F family members by cyclin-dependent kinases. *Mol. Cell. Biol.* **1997**, *17*, 3867−3875. (d) Okata, K.; Hisanaga, S.; Sugita, M.; Okuyama, A.; Murofushi, H.; Kitazawa, H.; Chari, S.; Bulinski, J. C.; Kishimoto, T. MAP4 is the in vivo substrate for cdc2 kinase in HeLa cells: identification of an M-phase specific and a cell cycle-independent phosphorylation site in MAP4. *Biochemistry* **1997**, *36*, 15873−15883.

(4) (a) Xiong, Y.; Hannong, G. J.; Zhang, H.; Casso, D.; Kobayashi, R.; Beach, D. p21 is a universal inhibitor of cyclin kinases. *Nature* **1993**, *366*, 701−704. (b) Lukas, J.; Parry, D.; Aagaard, L.; Mann, D. J.; Bartkova, J.; Strauss, M.; Peters, G.; Bartek, J. Retinoblastoma protein-dependent cell-cycle inhibition by the tumor suppressor p16. *Nature* **1995**, *375*, 503−506. (c) Polyak, K.; Kato, J. Y.; Solomon, M. J.; Sherr, C. J.; Massague, J.; Roberts, J. M.; Koff, A. p27Kip 1, a cyclin-dependent Cdk inhibitor, links transforming growth factor-beta and contact inhibition to cell cycle arrest. *Genes. Dev.* **1994**, *8*, 9−22.

(5) (a) Kamb, A.; Gruis, N. A.; Weaver-Feldhaus, J.; Liu, Q.; Harshman, K.; Tavtigian, S. V.; Stockert, E.; Day III, R. S.; Johnson, B. E.; Skolnik, M. H. A Cell Cycle Regulators, Potentially Involved in Genesis of Many Tumor Types. *Science* **1994**, *264*, 436−440. (b) Nobori, T.; Miura, K.; Wu, D. J.; Lois, A.; Takabayashi, K.; Carson, D. A. Deletions of the cyclin-dependent kinase-4 inhibitor gene in multiple human cancers. *Nature (London)* **1994**, *368*, 753−756. (c) Pines, J. Cyclins, CDKs and cancer. *Semin. Cancer Biol.* **1995**, *6*, 63−72. (d) Hartwell, L. H.; Kastan, M. B. Cell cycle control and cancer. *Science* **1994**, *266*, 1821−1828.

(6) (a) Webster, K. R. The therapeutic potential of targeting the cell cycle. *Exp. Opin. Invest. Drugs* **1998**, *7* (6), 1−23. (b) Rosania, G. R.; Chang, Y.-T. Targeting hyperproliferative disorders with cyclin dependent kinase inhibitors. *Exp. Opin. Ther. Patents* **2000**, *10*, 215−230. (c) Sielecki, T. M.; Boylan, J. F.; Benfield, P. A.; Trainor, G. L. Cyclin-Dependent Kinase Inhibitors: Useful Targets in Cell Cycle Regulation. *J. Med. Chem.* **2000**, *43*, 1−18.

(7) (a) Kaur, G.; Stetler-Stevenson, M.; Sebers, S.; Worland, P.; Sedlacek, H.; Myers, C.; Czech, J.; Naik, R.; Sausville, E. Growth Inhibition with Reversible Cell Cycle Arrest of Carcinoma Cells by Flavone L86-8275. *J. Natl. Cancer Inst.* **1992**, *84*, 1736−1740. (b) Carlson, B.; Dubay, M. M.; Sausville, E. A.; Brizuela, L.; Worland, P. J. Flavopiridol Induces G1 Arrest with Inhibition of Cyclin-dependent Kinase (CDK) 2 and CDK4 in Human Breast Carcinoma Cells. *Cancer Res.* **1996**, *56*, 2973−2978. (c) Sedlacek, H. H.; Czech, J.; Naik, R.; Kaur, G.; Worland, P.; Losiewicz, M.; Parker, B.; Carlson, B.; Smith, A.; Senderowicz, A.; Sausville, E. Flavopiridol (L868275; NSC649890), a new kinase inhibitor for tumor therapy. *Int. J. Oncol.* **1996**, *9*, 1143−1168

(8) (a) Kiriyama, N.; Nitta, K.; Sakaguchi, Y.; Taguchi, Y.; Yamamoto, Y. Studies on the Metabolic Products of *Aspergillus terreus*. III. Metabolite of the Strain IFO 8835. *Chem. Pharm. Bull.* **1977**, *25*, 2593−2601. (b) Kitagawa, M.; Okabe, T.; Ogino, H.; Matsumoto, H.; Suzuki-Takahashi, I.; Kokubo, T.; Higashi, H.; Saitoh, S.; Taya, Y.; Yasuda, H.; Ohba, Y.; Nishimura, S.; Tanaka, N.; Okuyama, A. Butyrolactone I, a selective inhibitor of cdk2 and cdc2 kinase. *Oncogene* **1993**, *8*, 2425−2432.

(9) (a) Vesely, J.; Havlicek, L.; Strnad, M.; Blow, J.; Donella-Deana, A.; Pinna, L.; Letham, D. S.; Kato, J.; Detivaud, L.; Leclerc, S.; Meijer, L. Inhibition of cyclin-dependent kinases by purine analogues. *Eur. J. Biochem.* **1994**, *224*, 771−786. (b) Abraham, R.; Acquarrrrone, M.; Andersen, A.; Asensi, A.; Belle, R.; Berger, F.; Bergounioux, C.; Brun, G.; Buquet-Fagot, C.; Fagot, D.; Glab, N.; Goudeau, H.; Goudeau, M.; Guerrier, P.; Houghton, P.; Hendriks, H.; Kloareg, B.; Lippai, M.; Marie, D.; Maro, B.; Meijer, L.; Mester, J.; Mulner-Lorillon, O.; Poulet, S.; Schierenberg, E.; Schutte, B.; Vaulot, D.; Verlhac, M. Cellular effects of olomoucine, an inhibitor of cyclin-dependent kinases. *Biol. Cell.* **1995**, *83*, 105−120 (c) Havlicek, L.; Hanus, J.; Vesely, J.; Leclerc, S.; Meijer, L.; Shaw, G.; Strnad, M. Cytokinin-Derived Cyclin-Dependent Kinase Inhibitors: Synthesis and cdc2 Inhibitory Activity of Olomoucine and Related Compounds. *J. Med. Chem.* **1997**, *40*, 408−412.

(10) Schultz, C.; Linj, A.; Leost, M.; Zaharevitz, D. W.; Gussio, R.; Sausville, E. A.; Meijer, L.; Kunick, C. Paullones, a Series of Cyclin-Dependent Kinase Inhibitors: Synthesis, Evaluation of CDK1/Cyclin B Inhibition, and in Vitro Antitumor Activity. *J. Med. Chem.* **1999**, *42*, 2909−2919.

(11) (a) Norman, T. C.; Gray, N. S.; Koh, J. T.; Schultz, P. G. A Structure-Based Library Approach to Kinase Inhibitors. *J. Am. Chem. Soc.* **1996**, *118*, 7430−7431. (b) Imbach, P.; Capraro, H.; Furet, P.; Mett, H.; Meyer, T.; Zimmermann, J. 2,6,9-Trisubstituted Purines: Optimization Towards Highly Potent and Selective CDK1 Inhibitors. *Bioorg. Med. Chem. Lett.* **1999**, *9*, 91−96. (c) Murthi, K. K.; Dubay, M.; McClure, C.; Brizuela, L.; Boisclair, M. D.; Worland, P. J.; Mansuri, M. M.; Pal, K. Structure−Activity Relationship Studies of Flavopiridol Analogues. *Bioorg. Med. Chem. Lett.* **2000**, *10*, 1037−1041.

(12) Vlahos, C. J.; Matter, W. F.; Kwan, Y. H.; Brown, R. F. A specific Inhibitor of Phosphatidylinositol 3-Kinase, 2-(4-Morpholinyl)-8-phenyl-4H-1-benzopyran-4-one (LY294002). *J. Biol. Chem.* **1994**, *269*, 5241−5248.

(13) (a) Kattige, S. L.; Naik, R. G.; Lakdawalla, A. D.; Alihussein, N. D.; Rupp, R. H.; Souza, N. J. 4H-Benzopyran-4-one Compounds Which Have Antiinflammatory Or Immunomodulating Action. U.S. Patent 4,900,727, Feb 13, 1990. (b) Naik, R. G.; Kattige, S. L.; Bhat, B.; Alreja, B.; Souza, N. J.; Rupp, R. H. An Antiinflammatory Cum Immunomodulatory Piperidinylbenzopyranone from *Dysoxylum Binectariferum*: Isolation, Structure and Total Synthesis. *Tetrahedron* **1988**, *44*, 2081−2086.

(14) Noyori, R.; Tokunaga, M.; Kitamura, M. Stereoselective Organic Synthesis via Dynamic Kinetic Resolution. *Bull. Chem. Soc. Jpn.* **1995**, *68*, 36−56.

(15) Structure determination protocols used for crystallography: Lawrie, A. M.; Noble, M. E. M.; Tunnah, P.; Brown, N. R.; Johnson, L. N.; Endicott, J. A. Protein kinase inhibition by staurosporine revealed in details of the molecular interaction with CDK2. *Nat. Struct. Biol.* **1997**, *4*, 796−801.

(16) Filgueira de Azevedo, W., Jr.; Mueller-Dieckmann, H.-J.; Schulze-Gahmen, U.; Worland, P. J.; Sausville, E. A.; Kim, S.-H. Structural basis for specificity and potency of a flavonoid inhibitor of human CDK2, a cell cycle kinase. *Proc. Natl. Acad. Sci. U.S.A.* **1996**, *93*, 2735−2740.

(17) Bairoch, A.; Apweiler, R. The SWISS-PROT protein sequence database and its supplement TrEMBL in 2000. *Nucleic Acids Res.* **2000**, *28*, 45−48.

(18) Losiewicz, M. D.; Carlson, B. A.; Sausville, E. A.; Nauk, R. G.; Narayanan, V. L.; Worland, P. J. Proceedings of the 88th Annual Meeting of American Association for Cancer Research, Toronto, Canada, 1995; p 35 (abstract).

(19) Burley, S. K.; Petsko, G. A. Amino-aromatic interactions in proteins. *FEBS Lett.* **1986**, *203*, 139−143.

(20) Schulze-Gahmen, U.; Brandsen, J.; Jones, H. D.; Morgan, D. O.; Meijer, L.; Vesely, J.; Kim, S.-H. Multiple modes of ligand recognition: Crystal structures of cyclin-dependent protein kinase 2 in complex with ATP and two inhibitors, olomoucine and isopentenyladenine. *Proteins Struct. Funct. Genet.* **1995**, *22*, 378−391.

(21) Howard, A. J.; Nielsen, C.; Xuong, N. H. Software for a Diffractometer with multiwire Area Detector. *Methods Enzymol.* **1985**, *114*, 452−472.

(22) Brünger, A. T.; Kuriyan, J.; Karplus, J. Crystallographic R-factor refinement by molecular dynamics. *Science* **1987**, *235*, 458−460.

JM000231G